REAL-TIME B-SCAN ULTRASONIC IMAGING USING A DIGITAL PHASED ARRAY SYSTEM FOR NDE

Robert Dunki-Jacobs and Lewis Thomas

General Electric Company
Schenectady, New York, 12301

INTRODUCTION

Phased array systems for electronically steering and focusing ultrasonic fields have been used extensively in medical imaging since the late 1970's. Despite the advantages of these systems (rapid redirection of beams, dynamic focusing to improve depth-of-field, and reduced mechanical complexity), phased arrays have been used very little for materials characterization. The reason for this lack of phased array technology in materials characterization is simply the wide range of velocity of sound encountered when working with materials and the resulting complexity in the beam former (the electronic system that appropriately delays and sums signals from individual elements of an array to produce a steered, focused beam) of a phased array system that can image in a wide variety of materials. Most medical phased array systems have analog beam formers which are hard-wired assuming the velocity of sound in soft tissue (1.54 mm/μsec), and therefore cannot be easily used to image in metals where the velocity of longitudinal sound waves is 3 or 4 times the velocity in soft tissue. At GE Corporate Research & Development (CRD) we have constructed a phased array system which uses a completely programmable digital beam former. This system provides exceptional flexibility for phased array imaging in a wide variety of materials; allowing focusing and steering using either the longitudinal or transverse wave velocity for any material.

DESCRIPTION OF PHASED ARRAY SYSTEM

All phased array systems can be described using the block diagram shown in Figure 1. The beam former module is responsible for transmitting a beam which is focused and steered to a desired depth and angle. This is achieved by pulsing transducer elements which are further from the desired focal zone first and pulsing elements which are close to the focal zone an appropriate time later such that the acoustic signals from each element arrive at the focal spot simultaneously and with the same phase. On receive, the beam former must also focus and steer the received beam. This is done by delaying the electrical signals from elements which are close to the focal spot and then summing the delayed electrical signals from all the elements to produce a focused and steered beam. However, unlike transmit where only one focal spot is possible, on receive the focus can be changed to focus at all depths as acoustic signals from those depths are received. This is possible because the time at which an acoustic echo is received is linearly related to the depth from which it originated by the velocity of sound. Therefore, immediately after the transmit pulse, the array is

Review of Progress in Quantitative Nondestructive Evaluation, Vol. 11
Edited by D.O. Thompson and D.E. Chimenti, Plenum Press, New York, 1992

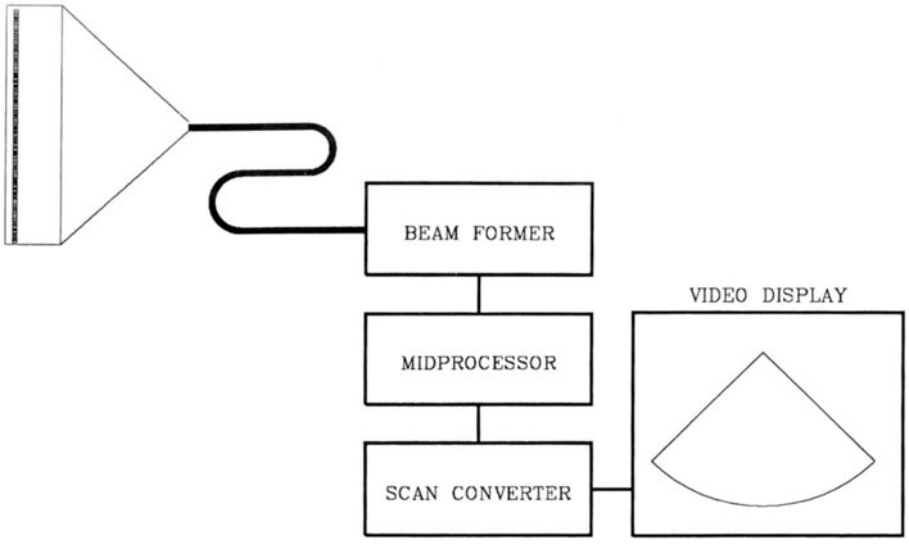

Figure 1. High level block diagram of a phased array imaging system.

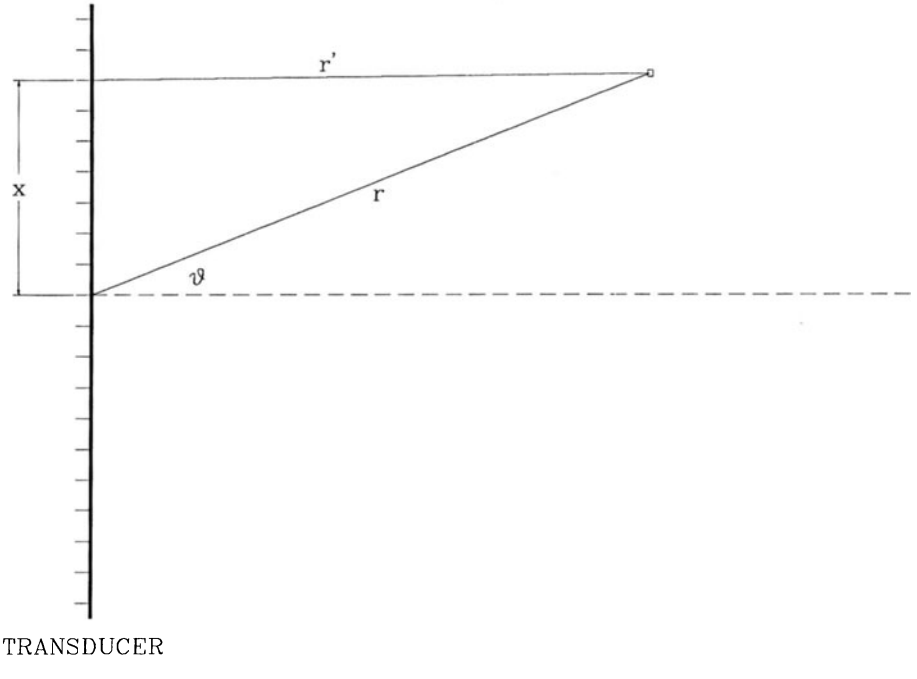

Figure 2. Drawing showing the geometry for determining the necessary time delays to steer and focus a phased array.

focused right in front of the transducer; as time goes on the delays in the beam former are changed to adjust the focus further away from the transducer as deeper and deeper echos are received. A drawing of the receive geometry and the beam former delays in shown in Figure 2.

Using the definitions of x, r, r', and θ provided in Figure 2 we now derive the time delay (Δt) for an element a distance x from the center of the array.

$$r' = [(rsin\theta - x)^2 + r^2cos^2\theta]^{1/2} \tag{1}$$

$$r' = r[1 + \frac{x^2 - 2rxsin\theta}{r^2}]^{1/2} \tag{2}$$

Expanding the square root and keeping terms of order x^2 and lower we obtain:

$$r' \approx r - xsin\theta + \frac{1}{2}\frac{x^2cos^2\theta}{r} \tag{3}$$

Therefore:

$$r - r' \approx xsin\theta - \frac{1}{2}\frac{x^2cos^2\theta}{r} \tag{4}$$

Finally, by dividing by the velocity of sound (v) we convert the difference in distance to the focal point to a time difference:

$$\Delta t \approx \frac{r - r'}{v} \approx \frac{xsin\theta}{v} - \frac{1}{2}\frac{x^2cos^2\theta}{vr} \tag{5}$$

The first term of the right-hand-side of equation (5) ($xsin\theta/v$) is often referred to as the steering term because it only varies with x and θ. In addition, if the transducer was unfocused (equivalent to focusing at infinite r) then only this first term would be present in the time-delay equation. The second term of the right-hand-side of equation (5) ($x^2cos^2\theta/2vr$) is called the focusing term. In addition to depending on x and θ, the focusing term also varies as $1/r$.

The midprocessor module shown in Figure 1 is responsible for taking the beam formed data and converting it to a video format. Usually this involves only video detection and scan conversion, however, if motion is present in the region insonified then the velocity of the motion can be determined using Doppler processing, which is also done in the mid-processor. Finally, the midprocessor passes the image data to a real-time display (typically an VGA monitor).

The phased array system constructed at CRD has been described in detail previously (O'Donnell et al. 1990). Briefly, it consists of a 96 channel digital beam former, which is interfaced to a conventional ultrasound imaging system (which performs midprocessor functions and real time display) and to a Biomation logic analyzer with enough memory to store 8 seconds of continuous data for off-line analysis.

Signals from each element of the array are first amplified and then digitized at a rate which exceeds the Nyquist sampling criterion for the highest frequency generated by the transducer. The digitized signals from the n^{th} element are then passed to a custom VLSI chip which appropriately delays the data and sums it with data from the $(n-1)^{th}$ element, passing the sum on to an identical chip attached to the $(n+1)^{th}$ element. The output of the 96th channel is the beam formed result, containing the full radio-frequency information (at baseband). This data is then passed on to the Biomation logic analyzer for off-line analysis and to a conventional ultrasound imager where video detection and scan conversion are performed before displaying the image in real-time.

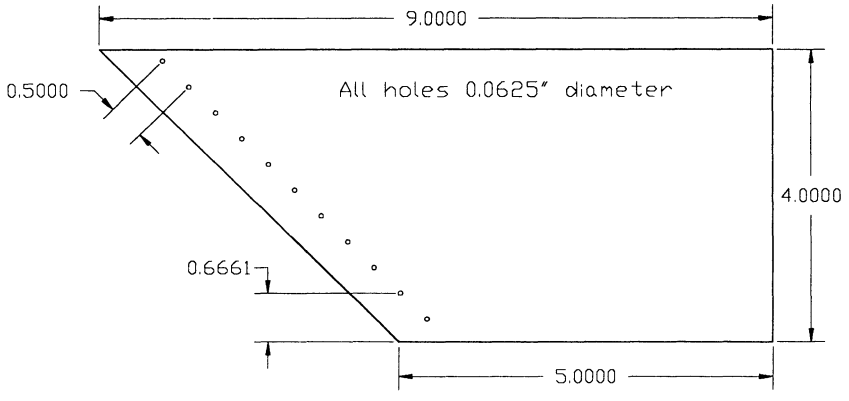

Figure 3. Drawing of sample #1.

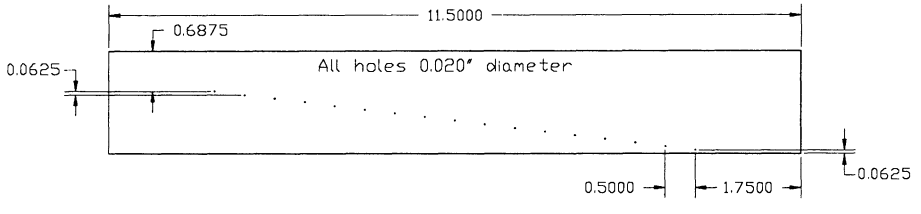

Figure 4. Drawing of sample #2.

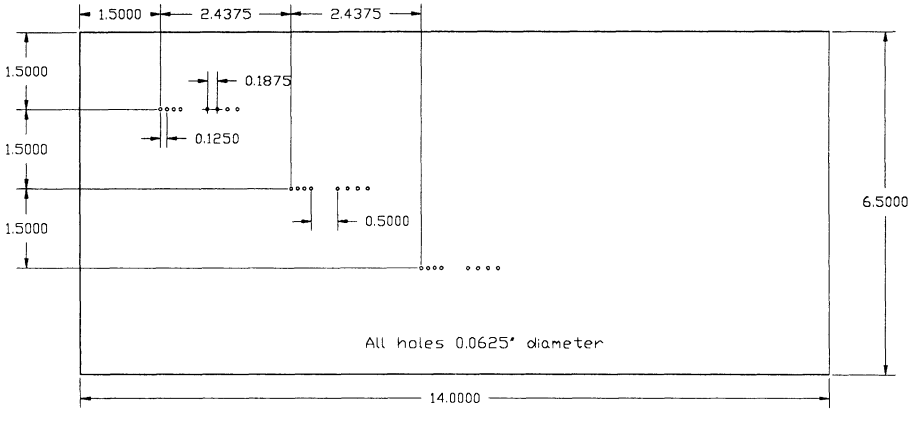

Figure 5. Drawing of sample #3.

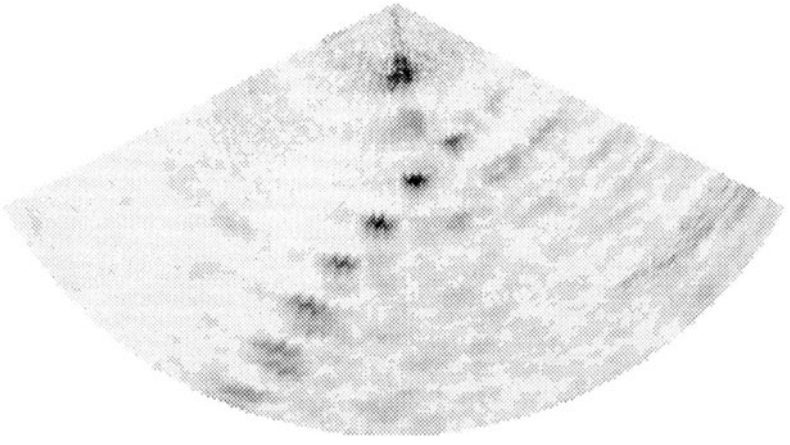

Figure 6. Grey-scale image of $1/16^{th}$ inch diameter side drilled holes, separated by one-half inch on a 45 degree angle. The velocity of sound used in the beam forming equations was 6 mm/μsec.

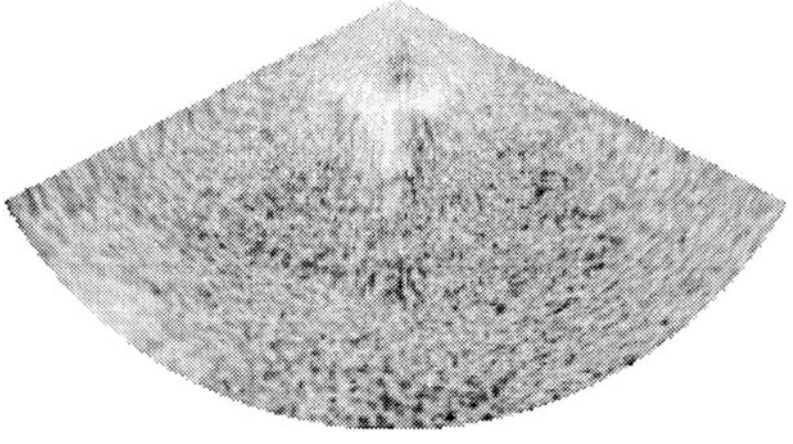

Figure 7. Image produced under identical circumstances to those in Figure 6 except that the velocity of sound used for the beam forming equations is 1.5 mm/μsec.

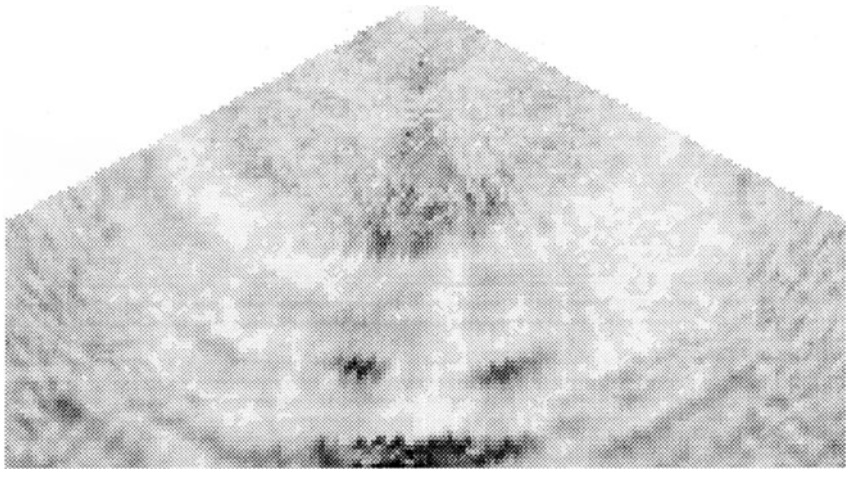

Figure 8. Grey-scale image of .020 inch side drilled holes.

EXPERIMENTAL CONDITIONS

Images of three different samples will be presented in this paper. All samples are made of Aluminum and the velocity of sound in each sample was measured to be approximately 6 mm/μsec. Drawings of the samples are presented in Figures 3 through 5. All studies were performed using a 3.75MHz center frequency transducer with approximately a 40% fractional bandwidth. The transducer has 96 elements, arranged as a linear array, and is approximately 1.5 cm square. All images were produced with the transducer in contact with the part being scanned. The images presented here are formed using 128 beams steered over a 123.5 degree sector. In order to focus the transducer in the direction perpendicular to the array dimension a mechanical lens is used which has a focal length of 6cm in water and a round-trip transit time of 4μsec. Reverberations from within this lens may be seen in most of the images presented here.

RESULTS

In Figures 6 and 7 we present two images of the block with $1/16^{th}$ inch side drilled holes spaced 0.5 inches apart on a 45 degree angle. Figure 6 was produced with the beam former programmed for a velocity of sound equal to that of longitudinal waves in Aluminum (6 mm/μsec), while Figure 7 was produced with the beam former programmed for a velocity of sound equal to that of water (1.54 mm/μsec). The holes are clearly visible as dark spots running along a 45 degree angle in the image in Figure 6, however, no evidence of the holes is seen in Figure 7. This degradation of the image due to beam forming using the wrong velocity of sound is due to two effects: defocusing and oversteering. Defocusing occurs because the dynamic focusing on receive is inappropriate. Since the ratio of the true velocity of sound to the programmed one is approximately 4, the beam former is using time delays appropriate for a depth which is only one-fourth the depth from which the echos actually originate. This effect can be easily seen by examining the focusing term of equation (5). The oversteering effect results in steering beams at greater angles from perpendicular to the material surface than was intended due to using the wrong velocity in the beam former. As can be seen from the steering term of equation (5), the ratio of the sine of the intended steering angle to the sine of the actual steering angle will be equivalent to the ratio of the actual velocity of sound to the velocity used in the beam former. This

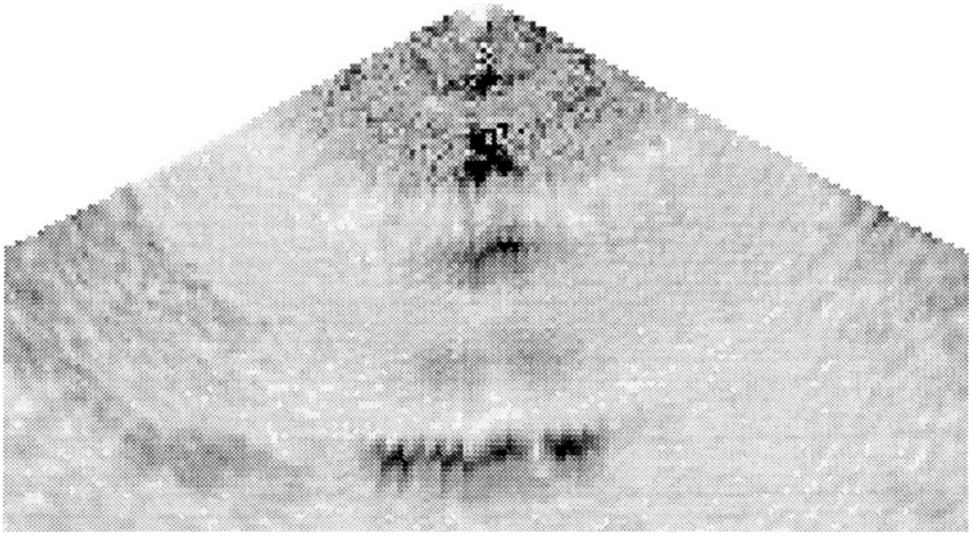

Figure 9. Grey-scale image of four holes $3/16^{th}$ of an inch apart.

Figure 10. Binary image of four holes $3/16^{th}$ of an inch apart. This image was produced by thresholding Figure 9 at 92% of the peak amplitude in the image.

results in significantly distorting the image at small steering angles (less than 15 degrees if the ratio of the actual velocity to the programmed velocity is 4) and for greater steering angles in a completely unfocused, unsteered beam.

In Figure 8 we show an image of the block with .020 inch side drilled holes. For this image the transducer was located such that the holes are approximately 1.5 inches deep. Two holes are evident in this image as dark spots near the bottom of the image (the dark streak at the bottom of the image is the back of the sample). In principle other holes should be visible in this image, however at large steering angles more sound is converted into shear waves in the sample, resulting in only weekly scattered signals at the time of arrival of longitudinal waves. At 3.75Mhz, the wavelength of sound in Aluminum is approximately .063 inches, therefore these holes represent scatterers that are only one-third of a wavelength in diameter.

In Figures 9 and 10 we present images of the $1/16^{th}$ inch diameter side drilled holes which are $3/16^{th}$ of an inch apart and 1.5 inches deep. Given the 15 mm aperture of our phased array transducer, the F number for imaging these holes is 2.5, while the holes are only 3 wavelengths apart. Although the grey-scale image presented in Figure 9 shows the echos from the holes overlapping into a single streak (near the bottom of the image), the binary image produced by thresholding at 92% of the maximum value in the image shows 4 distinct echos (see Figure 10). Note, the bright echos in the top half of Figures 9 and 10 are echos from the mechanical focusing lens.

DISCUSSION

In general, the results presented here demonstrate the capability of producing real-time images in metals using a phased array ultrasound system. In particular, the results presented in Figures 6 and 7 show how important having a very flexible, highly programmable beam former is. As is clearly shown by these results, using a phased array system which is designed to work only for medical imaging is not likely to produce pleasing results. The data presented on imaging .020 inch side drilled holes indicates the sensitivity of this system to small flaws; we will be extending this work in the future to real flaws. Finally, the images in Figures 9 and 10 indicate that the resolution of this imaging system is close to the theoretical capabilities given the aperture size and wavelength.

REFERENCES

1. M. O'Donnell, W.E. Engeler, J.T. Pedicone, A.M. Itani, S.E. Noujaim, R.J. Dunki-Jacobs, W.M. Leue, C.L. Chalek, L.S. Smith, J.E. Piel, R.L. Harris, K.B. Welles and W.L.Hinrichs (1990). Real-Time Phased Array Imaging Using Digital Beam Forming and Autonomous Channel Control, Proc. IEEE Ultrasonics Symp.